UCRL-ID-135402

Nickel and Manganese Interaction with Calcite

M. Zavarin
H. Doner

August 16, 1999

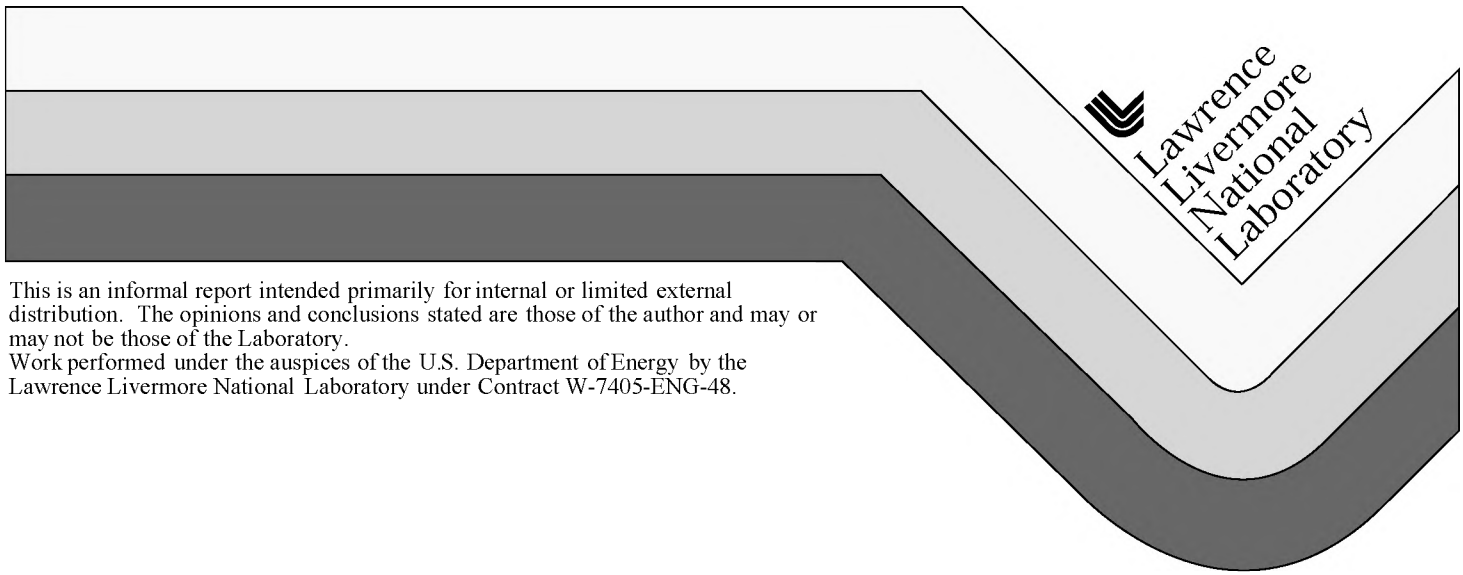

This is an informal report intended primarily for internal or limited external distribution. The opinions and conclusions stated are those of the author and may or may not be those of the Laboratory.
Work performed under the auspices of the U.S. Department of Energy by the Lawrence Livermore National Laboratory under Contract W-7405-ENG-48.

DISCLAIMER

This document was prepared as an account of work sponsored by an agency of the United States Government. Neither the United States Government nor the University of California nor any of their employees, makes any warranty, express or implied, or assumes any legal liability or responsibility for the accuracy, completeness, or usefulness of any information, apparatus, product, or process disclosed, or represents that its use would not infringe privately owned rights. Reference herein to any specific commercial product, process, or service by trade name, trademark, manufacturer, or otherwise, does not necessarily constitute or imply its endorsement, recommendation, or favoring by the United States Government or the University of California. The views and opinions of authors expressed herein do not necessarily state or reflect those of the United States Government or the University of California, and shall not be used for advertising or product endorsement purposes.

This report has been reproduced
directly from the best available copy.

Available to DOE and DOE contractors from the
Office of Scientific and Technical Information
P.O. Box 62, Oak Ridge, TN 37831
Prices available from (423) 576-8401

Available to the public from the
National Technical Information Service
U.S. Department of Commerce
5285 Port Royal Rd.,
Springfield, VA 22161

Proposal 2333

Nickel and Manganese Interaction with Calcite

Mavrik Zavarin[1] and Harvey E. Doner[2]

[1]Lawrence Livermore National Laboratory, Livermore, CA 94551
[2]University of California, Berkeley, CA 94720

Introduction

Many divalent metal cations sorb to calcite surfaces and incorporate into calcite to varying degrees. Since calcite may sorb trace elements in the environment, the factors controlling metal-calcite interactions are critical to understanding element cycling. The interaction of divalent metal cations with calcite can be critical to toxic metal immobilization[1], nutrient cycling, interpretation of past redox conditions[2], tracing fluid flow[3], for example.

Sorption of Ni and Mn on calcite surfaces was studied by Zachara et al.[4]. At any particular pH, the sorption of Mn on calcite was greater than Ni. This was attributed in part to the similarity of divalent Mn and Ca with respect to ion size. Although direct spectroscopic evidence was not available, sorption/desorption results suggested that Mn quickly forms a surface precipitate or solid solution while Ni forms a hydrated surface complex that may incorporate into calcite much more slowly via recrystallization. Because Mn(II) ionic radius is similar to that of Ca(II) (0.80 versus 1.0Å), and because $MnCO_3$ has a structure similar to calcite, it is likely that Mn can substitute directly for Ca in the calcite structure. The ionic radius of Ni(II) is significantly smaller (0.69Å) and $Ni(OH)_2$ precipitation is likely to be favored in most systems. For Ni, direct substitution for Ca is less likely or may require more significant calcite lattice deformation.

Materials and Methods

Ni and Mn sorption samples were prepared at beam line 4-3 at SSRL several hours prior to sample analysis. A range of solution metal concentrations were used (5-100 ppm) to investigate concentration effects. Since XAS detection limits are high, samples required approximately 50 ppm metal; thus, all sorption samples were supersaturated with respect to $Ni(OH)_2$ or $MnCO_3$. Coprecipitation samples were prepared using a pH-stat set-up run at 0.03% and 0.25% CO_2 and sodium chloride background electrolyte (I=0.1). In coprecipitation samples, solutions were always undersaturated with respect to all known Mn or Ni minerals. Although this did not eliminate the possibility of trace metal precipitation (surface precipitates have been shown to form when solution concentrations are below the solubility of the particular mineral), it reduced the likelihood of mineral precipitation and was a better representation of solution metal concentrations in the environment.

Results and Discussion

1. Ni(II) Sorption on Calcite

Figure 1 contains EXAFS data for aqueous, sorbed, and coprecipitated Ni on calcite. For all sorption samples, no significant change in spectra occurred as a function of time during data collection. This indicated that, within the first several hours of Ni sorption, no significant restructuring occurred at the calcite surface. The EXAFS (and XANES) of all sorption samples were significantly different from aqueous Ni samples. This difference is indicative of inner-sphere Ni sorption or formation of Ni precipitates. The EXAFS FT data for sorbed Ni samples contained a second neighbor feature at ~2.8Å (not corrected for phase shift). This feature was much smaller than that of $Ni(OH)_2$, indicating that simple $Ni(OH)_2$ formation did not occur.

The formation of surface multinuclear complexes with Ni was previously shown to occur in pyrophyllite sorption experiments[5]. Those experiments showed that multinuclear complexes formed well below the solubility product of $Ni(OH)_2$ and that the relative Ni-Ni coordination numbers increased with Ni loading. The increase in the second neighbor peak amplitude with increased loading was observed here as well. Formation of a $Ni(OH)_2$-like surface precipitate or $(Ni, Ca)CO_3$ near-surface solid solution is likely in our case.

Although sorption EXAFS data were noisy, fits were attempted for all samples. In all cases,

second neighbor fits were the same or better when fitting with Ni and not Ca. This suggests that Ni multinuclear complexes formed in these samples. In addition, σ^2 values for Ca fits were unreasonably low while those of Ni were similar to $Ni(OH)_2$ fit results. The Ni-Ni distance in sorption samples

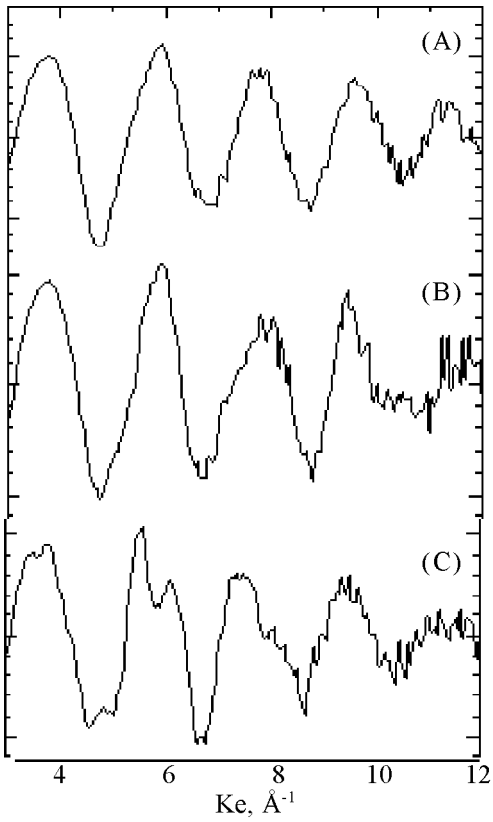

Figure 1. Ni EXAFS data of 100ppm aqueous Ni (A), 50 ppm Ni sorbed on calcite at pH 7.75 (B), and 500 ppb Ni coprecipitated in calcite (C) (EXAFS are K^3 weighted; relative amplitudes shown for y-axes).

also agreed with Ni-Ni distances in $Ni(OH)_2$. Second neighbors in sorption samples were, therefore, dominated by Ni atoms. The coordination number for Ni neighbors varied between 0.4 and 1.7, increasing with level of loading. When σ^2 was held at 0.0064 (average for $Ni(OH)_2$ sample), Ni coordination numbers varied between 0.6 and 1.6. The addition of a Ca shell in addition to a Ni shell improved the EXAFS fit significantly for all samples. Ni may, therefore, be found as a surface precipitate that coats the calcite surface. Since EXAFS data always represents the average coordination of an element, it is also possible that Ni was found in several coordination environments on the calcite surface. Some Ni atoms may have substituted for Ca near the calcite surface while another fraction was in a $Ni(OH)_2$-like coordination. At short times (~10 hours), either $Ni(OH)_2$-like multinuclear complexes or a mixture of $Ni(OH)_2$-like and Ni-substituted calcite species most likely formed in the presence of calcite.

2. Ni(II) Coprecipitation in Calcite

Ni XAS data for several coprecipitation samples were examined. The XANES were the same at all precipitation rates and pCO_2 but distinctly different from $Ni(OH)_2$, aqueous Ni, or sorbed Ni. The EXAFS and FTs were also different. Due to the complexity of the EXAFS, data fits were heavily constrained. For coprecipitation samples, data fits were initially constrained by assuming that Ni resides in the Ca position of calcite such that coordination numbers of atoms were held constant. Atom distances, σ^2, and S_0^2 were fit. For coprecipitation samples, with the addition of each shell of atoms, the fit improved and the first and second shell oxygen σ^2 values agreed with NiO fit results. Not all atoms in the nearest 5 Å from the Ca position were fit; 3 sets of 6 equivalent O atoms between 4 and 5Å were omitted to reduce the number of fitting parameters. Though the σ^2 for O at that distance was expected to be very high, a relatively poor fit between 3.5 and 4Å of the EXAFS FT could be attributed to those O atoms (Figure 2).

The coprecipitation data fits suggest that substitution of Ca for Ni in calcite results in the distortion of interatomic distances in the calcite lattice. The difference in atom distances (relative to ideal calcite) for the fitted atoms was -0.27, -0.10,
-0.09, -0.11, -0.07Å for increasingly distant back-scatterers (Figure 3). Thus, Ni substitution disturbed the atom lattice positions to at least 5Å. Though significant distortion of the calcite lattice occurred, EXAFS results indicate Ni substituted directly for Ca in calcite.

Since the ionic radius of Cu(II) is close to Ni(II) (0.73 and 0.69Å, respectively), EXAFS data was collected on coprecipitated Cu(II) and several standards. When coprecipitation data was fit using the same scheme as for Ni, the decrease in atom distance relative to calcite were -0.33, -0.20, -0.22, -0.11, and -0.06Å for increasingly distant neighbors. In the case of Cu, distortion of the calcite lattice occurred similar to Ni and distortion beyond 5Å was detectable. However, poor data fits for the Cu data indicated that, for Cu, symmetric distortion of the carbonate site most likely did not occur. Bond valence calculations indicated that octahedrally

coordinated O atoms at 2.03Å (fit result) were significantly too short for divalent Cu. This is likely due to the typical non-ideal octahedral coordination of Cu-O species that have 4 O at ~1.9Å and 2 at ~2.5Å. Both Ni and Mn usually have equidistant octahedral coordination and atom distances for coprecipitation samples are in agreement with bond-valence calculations.

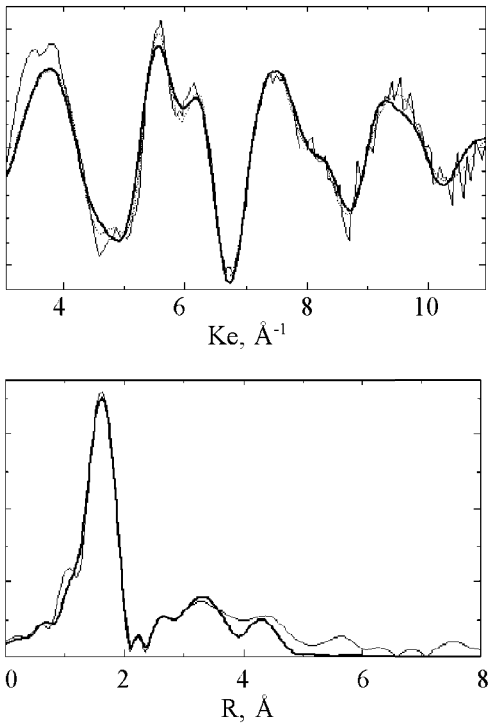

Figure 2. Data fit for Ni coprecipitation sample (solid line = data, dotted line = back-transform, thick line = back-transform fit; EXAFS and FT's are K^3 weighted; relative amplitudes shown for all y-axes).

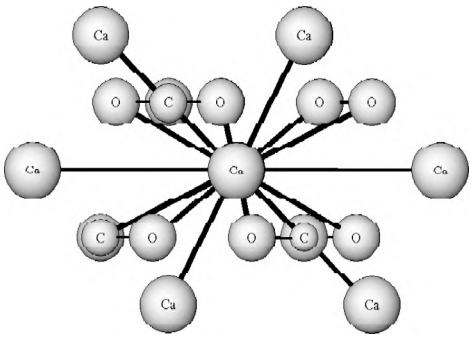

Figure 3. A diagram depicting the O, C, and Ca cluster of atoms that was fit in Ni coprecipitation EXAFS data.

3. Mn(II) Sorption on Calcite

For all sorption samples, Mn loading on calcite was low and EXAFS data fitting could not be accomplished. Though Mn sorbs more strongly to calcite than Ni, the Mn detection limits were significantly higher. Nevertheless, XANES data indicated that sorbed Mn was not dominated by an aqueous or $MnCO_3$-like species. Mn(II) sorption data was time-dependent during the period of XAS data collection. When examining the XANES as a function of time, the spectrum shape changed as a function of time (Figure 4). Each sorption scan is an average of several scans that represent approximately 2 hours of reaction time. For this sample, XAS data collection began after only a few hours of sorption. The first scan looks most like aqueous Mn(II) (or, possibly surface sorbed Mn(II)). The formation of additional XANES peaks as a function of time (and other EXAFS evidence) suggests a fast transformation from Mn sorption to solid solution formation (compare with Mn coprecipitation XANES).

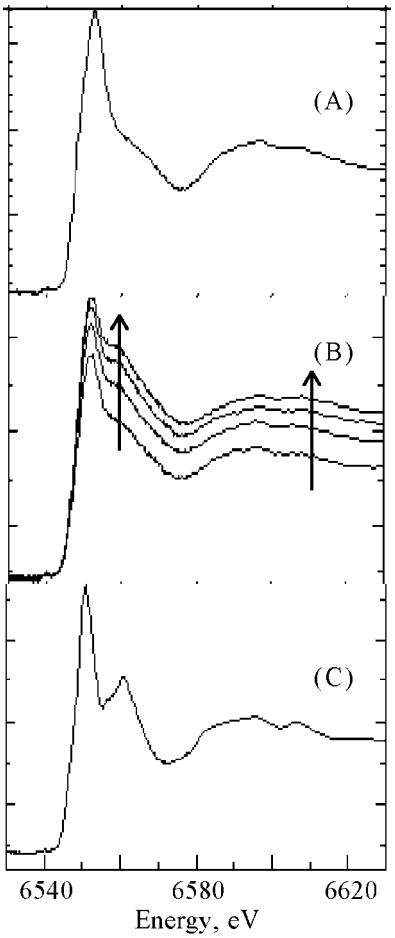

Figure 4. Mn XANES of 100 ppm aqueous Mn(II) (A), Mn(II) sorbed on calcite at pH 7.75, I = 0.1, 0.03% CO_2 (B), and 500 ppb

Mn(II) coprecipitated at 0.03% CO_2 and Ω = 3 (C) (relative amplitudes shown on y-axes; arrows indicate time trend).

Additional Mn sorption data suggested that, unlike Ni that formed a stable $Ni(OH)_2$ surface precipitate, Mn(II) interaction with calcite was a function of time and solution concentration. At low Mn(II) concentrations, Mn was found on calcite with a structure similar but not identical to Mn-substituted calcite; Mn was most likely substituting for Ca at the calcite surface or was quickly incorporated to form a solid solution in calcite. At higher Mn(II) concentrations, Mn formed a surface precipitate evidenced by Mn-Mn back-scattering. Within several hours, Mn(II) began to form a solid solution in calcite via diffusion through the hydrated calcite layer or calcite recrystallization, finally forming a structure similar to Mn substituted calcite. These EXAFS results provide direct evidence for the model described by Davis et al.[6] where sorption was described as a 2-step process of surface sorption followed by solid solution formation through surface recrystallization. The results also agree with Mn sorption observations of Zachara et al.[4] that indicated irreversible Mn sorption on calcite; the irreversible nature of Mn(II) sorption was most likely due to incorporation beyond the surface of calcite. The difference in reactivity of Ni and Mn sorption can be related to the relative ease of Mn dehydration compared to Ni (i.e. Mn dehydrates and can then substitute for Ca in calcite while Ni remains largely at the surface)[4].

4. Mn(II) Coprecipitation in Calcite

Several Mn(II) coprecipitation samples were examined using XAS. Precipitation rate and pCO_2 in the ranges examined did not affect the structure of Mn in calcite. The XANES contained 2 peaks near 6600 eV similar to the XANES of Mn sorption samples (Figure 4). These XANES were also significantly different from $MnCO_3$. The EXAFS FT data contained multiple features as in Ni and Cu coprecipitation results. The Mn coprecipitation EXAFS FTs were quite similar to $MnCO_3$ data though conspicuously different. A comparison of EXAFS data led to the same conclusion: though many of the features in coprecipitated Mn and $MnCO_3$ are similar, there are distinct difference between the spectra.

Data fits for coprecipitation samples showed similar changes in atoms distances as Ni and Cu coprecipitation results, though the effects were much slighter since Mn and Ca ionic radii are similar (Mn(II) = 0.8Å and Ca(II) = 1.0Å). Consequently, the distortion of fitted atoms distances relative to Ca positions in calcite were -0.14, -0.03, -0.07, -0.05, +0.01 for the nearest 5 fitted atom shells. In the case of Mn coprecipitation, distortion of calcite did not reach the second shell of Ca atoms and was slight beyond the first shell of O atoms. Although the fits assumed that no Mn was present in the first or second shell of divalent cation sites, this may not necessarily be the case. When fits were made with Mn instead of Ca back-scatterers, the fits were worse and fitted σ^2 values were too large. Nevertheless, a fraction of first or second shell divalent cation sites may contain some Mn atoms. This same argument could be made for Ni coprecipitation samples.

References

1. Doner, H. E. & Zavarin, M. in *Soils and Environment - Soil Processes from Mineral to Landscape Scale* (eds. Auerswald, K., Stanjek, H. & Bigham, J. M.) (Catena Verlag, 1996).
2. Dromgoole, E. L. & Walter, L. M. Inhibition of calcite growth rates by Mn^{2+} in $CaCl_2$ solution at 10, 25, and 50C. *Geoch. et Cosmoch. Acta* **5**, 2991-3000 (1990).
3. Kopp, O. C., D.K. Reeves, M. L. Rivers, and J.V. Smith. Synchrotron X-ray fluorescence analysis of zoned carbonate gangue in Mississippi Valley-type deposits. *Chemical Geology* **81**, 337-347 (1990).
4. Zachara, J. M., Cowan, C. E. & Resch, C. T. Sorption of divalent metals on calcite. *Geoch. et Cosmoch. Acta* **55**, 1549-1562 (1991).
5. Scheidegger, A. M., Lamble, G. M. & Sparks, D. L. in *Contaminated Soils: Third International Conference on the Biogeochemistry of Trace Elements* (ed. Prost, R.) D:\data\communic\011.PDF (INRA Editions, Paris, France, 1995).
6. Davis, J. A., Fuller, C. C. & Cook, A. D. A model for trace metal sorption processes at the calcite surface; adsorption of Cd^{2+} and subsequent solid solution formation. *Geoch. et Cosmoch. Acta* **51**, 1477-1490 (1987).